








RESEARCH

Open Access

The evaluation of non-anesthetic computed tomography for detection of pulmonary parenchyma in feline mammary gland carcinoma: a preliminary study



Auraiwan Klaengkaew¹ , Somchin Sutthigran¹ , Ninlawan Thammasiri¹ , Kittiporn Yuwatanakorn¹ ,
Chutimon Thanaboonnipat¹ , Suppawiwat Ponglowhapan²  and Nan Choisunirachon^{1*} 

Abstract

Background: Thoracic radiography in awake cats is a common procedure for the evaluation of pulmonary metastasis in feline mammary gland carcinoma (MGC). However, due to poor sensitivity, computed tomography (CT) is progressively taking its place. To perform CT in animals, general anesthesia is normally preferred but can cause lung atelectasis, affecting lung interpretation. Besides, MGC is often found in senile cats that are concurrently affected with other diseases, increasing anesthetic risk. Therefore, this study was aimed at comparing the effect of anesthesia on lung atelectasis observed through CT in clinically healthy cats and comparing the feasibility of non-anesthetic CT with non-anesthetic radiography in the detection of lung lesions in feline MGC. Thoracic CTs from anesthetized, clinically healthy cats and non-anesthetized either clinically healthy cats or MGC-affected cats were reviewed. In clinically healthy cats, motion artifacts and characteristics of lung atelectasis were observed and compared. In MGC-affected cats, motion artifacts were observed and compared to clinically healthy cats, and the number of MGC-affected cats, the number and characteristics of lung lesions were compared between non-anesthetic thoracic CT and radiography.

Results: Anesthesia significantly increased lung CT attenuation ($P = 0.0047$) and was significantly correlated with lung atelectasis (OR = 15; CI 2.02–111.18; $P = 0.0081$), particularly of the cranial lung lobe. Nonetheless, significantly higher motion artifacts in the caudal thoracic area were found in non-anesthetized healthy cats ($P = 0.0146$), but comparable low motion artifacts were observed in anesthetized healthy and MGC-affected cats. Non-anesthetic CT revealed higher numbers of MGC-affected cats and pulmonary nodules with a significantly lower nodular diameter ($P = 0.0041$) than those observed on radiographs. The smallest nodular diameters detected on radiographs and CT were 2.5 and 1.0 mm, respectively. Furthermore, CT showed additional information such as intra-thoracic lymphadenopathy, that could not be seen on radiographs.

* Correspondence: nan.c@chula.ac.th

¹Department of Surgery, Faculty of Veterinary Science, Chulalongkorn University, 39 Henri-Dunant Road, Wangmai, Pathumwan, 10330 Bangkok, Thailand

Full list of author information is available at the end of the article



© The Author(s). 2021 **Open Access** This article is licensed under a Creative Commons Attribution 4.0 International License, which permits use, sharing, adaptation, distribution and reproduction in any medium or format, as long as you give appropriate credit to the original author(s) and the source, provide a link to the Creative Commons licence, and indicate if changes were made. The images or other third party material in this article are included in the article's Creative Commons licence, unless indicated otherwise in a credit line to the material. If material is not included in the article's Creative Commons licence and your intended use is not permitted by statutory regulation or exceeds the permitted use, you will need to obtain permission directly from the copyright holder. To view a copy of this licence, visit <http://creativecommons.org/licenses/by/4.0/>. The Creative Commons Public Domain Dedication waiver (<http://creativecommons.org/publicdomain/zero/1.0/>) applies to the data made available in this article, unless otherwise stated in a credit line to the data.

Conclusions: Despite the motion artifacts, CT without anesthesia is a sensitive technique as it provides better lung inflation. Furthermore, compared to non-anesthetic radiography, non-anesthetic CT provided more information such as higher number of pulmonary nodules of a smaller size, including more distinct intra-thoracic lesions, such as lymphadenopathy, in MGC-affected cats.

Keywords: Atelectasis, Cat, Computed tomography, Lung, Mammary gland carcinoma, Radiography

Background

Mammary gland carcinoma (MGC) is the third most frequent feline neoplasms [1, 2]. It has been reported that MGC usually occurs in senile, female cats with an age ranging between 10 and 14 years [3, 4]. Due to aggressive biological behaviors, feline MGC normally demonstrates rapid growth and commonly metastasizes to regional lymph nodes and lungs [5, 6]. The survival period of feline MGC has been reported as being less than 6–12 months [5, 6]. Therefore, early diagnosis and accurate clinical staging observed through metastatic condition are essential for therapeutic planning and prognosis of feline MGC [1].

Diagnostic imaging is a non-invasive method for identification of MGC metastases. Radiography is an initial procedure for lung metastatic screening. Despite being a cheap, low radiation and generally applicable option, it has been reported in dogs that radiographs showed less sensitivity in detecting lung lesions both of size and number [7, 8]. However, to our knowledge, this information has not yet been explored in cats. Computed tomography (CT) is currently described as a superior modality in detecting lung lesions in dogs and cats [8–10]. CT has a higher ability to detect a smaller nodule without superimposition than radiographs in dogs [8]. To perform CT in animals, general anesthesia is usually required. However, general anesthesia can be a risk for respiratory compromised, feline patients [11]. Since feline MGC is commonly found in senile cats. These cats may be concurrently affected with other diseases increasing anesthetic risk such as cardiac or renal diseases. In addition, it has been suggested that anesthesia could prolong the duration of the CT procedure and it more importantly, caused lung atelectasis as seen in humans and cats [9, 12, 13].

As there is no information on the use of pulmonary CT, especially non-anesthetic CT for detecting lung metastases in feline MGC. Therefore, the objectives of this study were: (i) to evaluate the effect of anesthesia on the pulmonary appearance of healthy cats by means of the motion artifact and lung characteristic; and (ii) to compare the diagnostic feasibility between non-anesthetic CT and non-anesthetic radiographs for detecting lung lesions in MGC-affected cats. The hypotheses were that anesthesia can influence the appearance of lung parenchyma of healthy cats by means of the motion artifact and lung atelectasis, and non-anesthetic CT is superior

to non-anesthetic radiographs for detecting MGC metastatic lung lesions in terms of number, location and distinctness.

Results

Clinical demographic data

The number of attending cats in this study were 12, 12 and 20 cats for group (Gr.) 1 (the anesthetized healthy cats), Gr. 2 (the non-anesthetized healthy cats) and Gr. 3 (MGC-affected cats), respectively. All information concerning cats in each group are reported in Table 1. Gr. 1 and Gr. 2 had a significantly lower age than Gr. 3 ($P < 0.0001$ and $P = 0.017$, respectively) but the age between Gr.1 and Gr.2 and the body weight (BW) among groups were comparable ($P = 0.2522$ for age between Gr.1 and Gr. 2 and $P = 0.7434$ for BW among groups).

Motion artifacts on computed tomographic images

The number of cats and degree of motion artifacts observed on CT among groups are shown in Table 2. In Gr. 1 and Gr. 2, motion artifacts were detected at the caudal area of the thoracic cavity. In Gr. 3, nine cats revealed motion artifacts at the caudal thoracic area whereas one cat showed a motion artifact at the cranial part. Gr.1 and Gr. 3 had significantly less motion artifacts than Gr. 2 ($P = 0.0146$ and $P = 0.0246$, respectively) but motion artifacts between Gr. 1 and Gr. 3 did not differ significantly ($P > 0.9999$).

Lung atelectasis of healthy cats on computed tomographic images

Information on lung atelectasis such as the number of cats, number of lungs, average attenuation number and characteristics among normal lung tissue (NL), poorly lung aeration (PA) and non-lung aeration (NA) clinically healthy cats in Gr. 1 and Gr. 2 were reported and are compared in Table 3. At NL, there was no difference in lung attenuation between groups ($P = 0.1089$). Whereas at PA or NA, Gr.1 had a significantly higher attenuation number than that of the Gr. 2 ($P = 0.0047$). Considering the location, the most frequent locations of lung atelectasis were found at the right cranial lung (RtCr), the right middle lung (RtMd) and the cranial part of left cranial lung (LtCrCr) lobes, especially at the ventral area, and the peri-bronchial area was the common intra-parenchymal location (Table 4). There was a significant

Table 1 Clinical demographic data of clinically healthy cats, which divided into the anesthetized healthy cats (Gr. 1) and non-anesthetized healthy cats (Gr. 2), and mammary gland carcinoma affected cats (Gr. 3)

Parameters	Gr. 1	Gr. 2	Gr.3
Number	12	12	20
Age (months)	19.3 ± 23.6 ^a (7.0–84.0)	41.0 ± 10.8 ^a (24.0–60.0)	131.2 ± 41.0 ^a (24.0–216.0)
Body weight (kg)	3.4 ± 0.9 ^β (1.5–4.7)	3.6 ± 0.8 ^β (2.0–5.0)	3.7 ± 0.8 ^β (2.2–5.0)
Sex*			
Male	5	6	-
Intact	3	-	-
Castrated	2	6	-
Female	7	6	20
Intact	3	-	5
Spayed	4	6	15*
Breed			
Domestic short hair	9	7	16
Mixed breed	2	2	-
American short hair	-	2	-
British short hair	-	1	-
Scottish fold	1	-	-
Persian	-	-	4

* Sex and gonadal status of the cat at the experiment date
^aAge was compared among groups using Kruskal-Wallis test: $P < 0.0001$.
^aAge was compared between groups using Dunn’s Multiple comparisons test:
 Gr. 1 vs. Gr. 2: $P = 0.2522$.
 Gr. 1 vs. Gr. 3: $P < 0.0001$.
 Gr. 2 vs. Gr.3: $P = 0.0017$.
^βBody weight was compared among group using one-way ANOVA: $P = 0.7434$

Table 2 The motion artifact among anesthetized healthy cats (Gr. 1), non-anesthetized healthy cats (Gr. 2) and mammary gland adenocarcinoma affected cats (Gr. 3) on thoracic computed tomography

Group	Number of cats			Average motion artifact score
	Grade 0	Grade 1	Grade 2	
Gr. 1	8/12 (66.7 %)	3/12 (25.0 %)	1/12 (8.3 %)	0.4 ± 0.6
Gr.2	2/12 (16.6 %)	5/12 (41.7 %)	5/12 (41.7 %)	1.2 ± 0.7
Gr. 3	10/20 (50.0 %)	10/20 (50.0 %)	0/20 (0 %)	0.5 ± 0.5

Motion artifacts were compared among groups using Kruskal-Wallis test: $P = 0.0083$
 Motion artifacts were compared between groups using Dunn’s Multiple comparisons test:
 Gr. 1 vs. Gr. 2: $P = 0.0146$.
 Gr. 1 vs. Gr. 3: $P > 0.9999$.
 Gr. 2 vs. Gr.3: $P = 0.0246$

association between anesthetic procedure and the presence of lung atelectasis (OR = 15; CI 2.02–111.18; $P = 0.0081$).

Comparison of feline mammary gland carcinoma and pulmonary lesions between on non-anesthetic thoracic radiograph and on computed tomography

The radiographic and CT lung information such as number of cats, lesion distribution, lesion pattern, number of nodules, location, and size are reported in Table 5. Despite poor margination of detected nodules, CT unveiled images of nodule distinctness clearer than those observed on radiographs (Fig. 1 A-C). Lung nodules could not be detected on radiographs in three cats and those nodules were smaller than 2.5 mm. Radiographically, there was one cat affected by the left caudal lung lobe (LtCa) consolidation without a pulmonary nodule (Fig. 2 A and 2 C). However, on CT, this cat was later noted as having pulmonary nodules and the previous lung consolidation was noted as having moderately decreased lung volume with an alveolar pattern that was suspected to be atelectatic area (Fig. 2B and D). CT can significantly detect lesser diameter pulmonary nodules

Table 3 The number of cats, the number of lungs, average attenuation number and characteristics of atelectatic lung (HU) in anesthetized healthy cats (Gr. 1) and non-anesthetized healthy cats (Gr. 2)

Parameters	Gr. 1*	Gr.2*
Number of atelectatic cats	10/12 (83.3 %)	3/12 (25.0 %)
Normal lung		
Number of lung lobes	60/84 (71.4 %)	80/84 (95.2 %)
Attenuation number (HU)	-698.4 ± 71.9 (-678.1 to -721.2)	-666.3 ± 56.0 (-554.6 to -731.1)
Atelectatic lung		
Total number of lung lobes	24/84 ^a (28.5 %)	4/84 ^a (4.7 %)
Total attenuation number (HU)	-126.0 ± 70.2 (-39.7 to -364.3)	-381.5 ± 135.8 (-215.4 to -426.9)
-Poorly aerated lung tissue	22/84 (26.2 %)	4/84 (4.7 %)
Attenuation number (HU)	-174.0 ± 27.8 (-120.7 to -364.3)	-381.5 ± 135.8 (-215.4 to -426.9)
-Non-aerated lung	2/84 (2.3 %)	0/84 (0 %)
Attenuation number (HU)	-49.5 ± 13.8 (-39.7 to -59.3)	0
Characteristics		
-Peripheral		
Number of lung lobes	7/24 (29.2 %)	1/4 (25.0 %)
-Diffused		
Number of lung lobes	1/24 (4.2 %)	3/4 (75.0 %)
-Peribronchial		
Number of lung lobes	16/24 (66.6 %)	0/4 (0 %)
Locations		
-Dorsal	6/24 (25.0 %)	1/4 (25.0 %)
-Ventral	17/24 (70.8 %)	0/4 (0.0 %)
-Diffused	1/24 (4.2 %)	3/4 (75.0 %)

*The total number of cats and total number of lung lobe in each group were 12 and 84, respectively

^aThe association between anesthetic procedure and the presence of lung atelectasis was evaluated using the odds ratio: (OR = 15; CI 2.02–111.18; $P = 0.0081$)

than thoracic radiographs ($P = 0.0041$). In addition, five cats showed sternal lymphadenopathy only on CT, but not on radiographs.

Discussion

The precise evaluation of clinical staging is an important factor to indicate the proper therapeutic methods and precise prognosis in several malignancies including feline MGC [4, 6]. Although several studies in dogs and cats have reported that CT was more precise and provided additional diagnostic information of thorax compared to thoracic radiography [7–9], general anesthesia during the CT procedure can be one of the life-threatening risks to senile, MGC-affected cats that may have other

underlying impairments such as renal or cardiac diseases. Therefore, non-anesthetic CT for evaluation of pulmonary nodules could provide more safer and sensitive information for MGC-affected cats.

Anesthesia can cause lung atelectasis which interferes with the precision of lung evaluation in feline patients [9]. Characteristics of lung atelectasis in animals can include an interstitial or alveolar pattern [14]. Both patterns can mislead the diagnosis of pathologic lung lesions. A previous study in humans indicated that lung atelectasis appears on CT within five minutes following induction of anesthesia [15]. Similarly, in dogs, lung attenuation on CT was altered within three to eight minutes of anesthesia [16, 17]. In addition, it has been

Table 4 Distribution of poor pulmonary inflation in all affected cats (*n* = 13 cats) and each group of anesthetized healthy cats (Gr. 1) and non-anesthetized healthy cats (Gr. 2)

Lung atelectasis	Locations						
	RtCr	RtMd	RtAcc	RtCa	LtCrCr	LtCrCa	LtCa
Total affected cats	9	7	0	4	2	6	0
Poorly-aerated lung	7	7	0	4	2	6	0
-Gr.1	5	7	0	4	1	5	0
-Gr.2	2	0	0	0	1	1	0
Non-aerated lung	2	0	0	0	0	0	0
-Gr.1	2	0	0	0	0	0	0
-Gr.2	0	0	0	0	0	0	0

reported in human medicine that age and BW influence lung volume and oxygenation impairment. These impairments are higher with increased age or body mass index [18, 19]. However, the effect of these factors on lung volume and oxygen impairment in cats has never been documented. Due to the non-significant differences of age and BW between clinically healthy cats and lung

atelectasis in this study, the evidence of lung atelectasis in clinically healthy cats might be influenced by anesthetic procedure. Nevertheless, further studies that evaluate an effect of age or BW on lung volume in healthy cats under a control anesthetic protocol would provide additional information.

Motion artifacts were higher in non-anesthetized cats that had a normal respiratory rate of 20–30 breaths/min compared to anesthetized cats that maintained the anesthetic condition using a control ventilator at 12 breaths/min. The prolongation of respiration by a ventilator comparing to that of the cats with consciousness could eliminate motion artifacts. Despite a higher respiratory rate, non-anesthetized cats revealed a moderate motion artifact score that may affect diagnostic quality [20], especially at the caudal lung lobes suggesting the motion of the diaphragm [9].

In this study, anesthetized cats had significantly higher lung atelectasis than non-anesthetized cats in line with previous studies in dogs [21]. Lung atelectasis in cat may be caused by lung compression similar to human report [22]. Moreover, inhalation anesthesia was suggested in

Table 5 The radiographic and computed tomographic lung information such as the number of cats, lesion distribution, lesion pattern, the number of nodules, location, and size in twenty mammary gland adenocarcinoma affected cats

Lung metastasis	Radiograph	Computed tomography
Number of cats	7/20 (35.0 %)	10/20 (50.0 %)
Distribution of nodules		
Focal lesion	4/7 (57.1 %)	3/10 (30.0 %)
Diffuse lesion	3/7 (42.9 %)	7/10 (70.0 %)
Lesional pattern		
Ill-defined nodules	7/20 (35.0 %)	10/20 (50.0 %)
Lung consolidation without a nodule	1/20 (5.0 %)	0/20 (0 %)
Number of nodules	16	65
Location of nodules		
Right cranial compartment	2/16 (12.5 %)	11/65 (16.9 %)
Right middle compartment	5/16 (31.2 %)	8/65 (12.3 %)
Right caudal compartment	3/16 (18.7 %)	20/65 (30.7 %)
Left cranial compartment	0/16 (0 %)	7/65 (10.7 %)
Left middle compartment	0/16 (0 %)	6/65 (9.2 %)
Left caudal compartment	6/16 (37.5 %)	13/65 (20.0 %)
Size of nodules (mm)	5.8 ± 2.2 (2.5–10.2)	3.8 ± 1.9 (1.0–8.4)

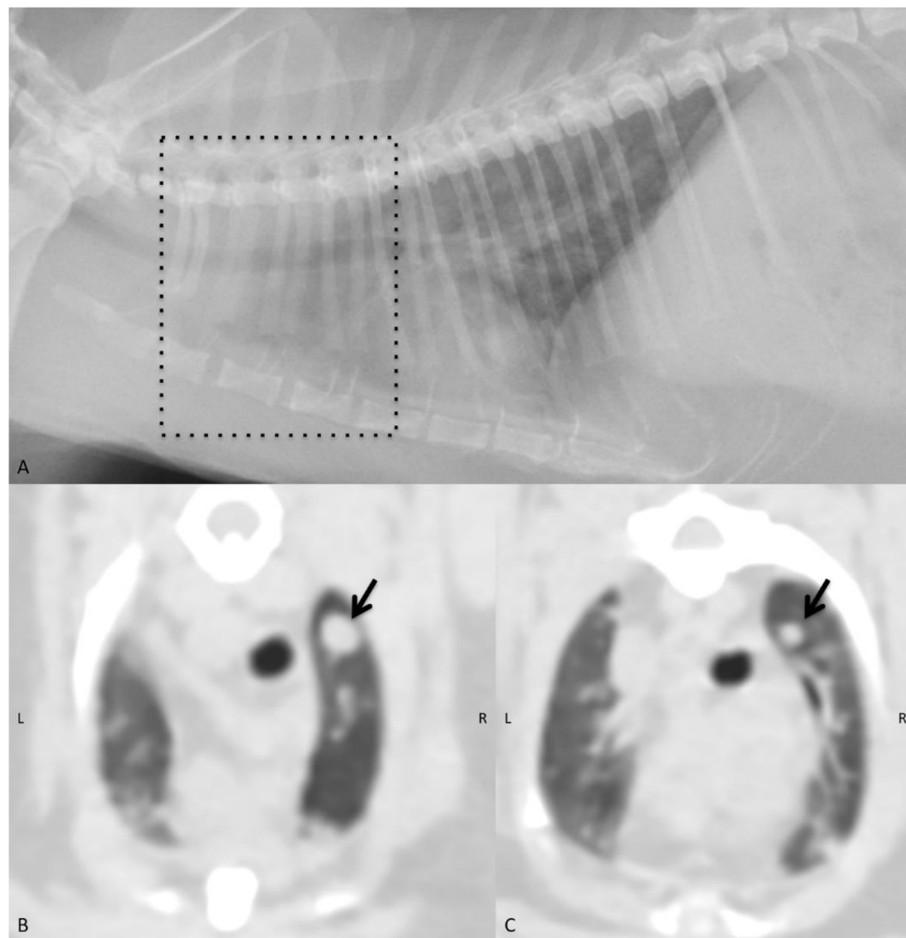


Fig. 1 A left lateral thoracic radiograph (A) and transverse computed tomographic image (B and C) of a mammary gland carcinoma affected cat. On radiograph (A), non-distinct ill-defined pulmonary nodules were found throughout the right inflated lung lobe. However, on transverse computed tomographic image (B and C), all pulmonary nodules, especially at the cranial thoracic compartment as seen on the thoracic radiograph (dash box, A) revealed clearly nodal margination (arrows)

human medicine as being one of the factors inducing atelectasis by the reduction of functional residual capacity due to the impairment of intercostal muscle function and the reduction of thoracic wall traction [22]. Besides, the lack of spontaneous deep inspiration phase resulting in the decrease of lung surfactant has also been noted [23]. The cranial displacement of the diaphragm by the increasing abdominal pressure during anesthesia in humans was reported to may increase the risk of atelectasis due to the decreasing thoracic cavity volume [24]. In addition to the anatomical factors during anesthesia, the administration of 100 % oxygen for carrying anesthetic gas may also cause lung atelectasis. Previous studies in dogs and cats reported that the higher oxygen concentration during general anesthesia was associated with a significantly increased degree of lung atelectasis [10, 21, 25, 26]. It has been reported that the 100 % oxygen for carrying anesthetic gas during the inhalation anesthesia induced more lung atelectatic

formation in cats than those who received the 40 % oxygen [10, 26].

The main atelectatic location in a previous feline study was reported as being distributed at a caudal lung lobe, close to the diaphragm [26]. However, the most frequent atelectatic locations in this study were found at the ventral portions of the RtCr, RtMd, and LtCrCr which are almost similar to another feline report [27]. The discrepancy among studies may be due to the compression force from the abdominal organs associated with the use of muscle relaxants during general anesthesia [26], whereas the atelectasis in the present study may be due to a smaller lung volume compared to other areas. A reduction of ventilation in the small lung lobes of cats can cause atelectatic development during general anesthesia similar to dogs [28]. Many atelectatic lungs revealed a peri-bronchial pattern at the ventral portion of the lung lobe. Therefore, utilization of CT as a diagnostic modality for pulmonary diseases, especially the

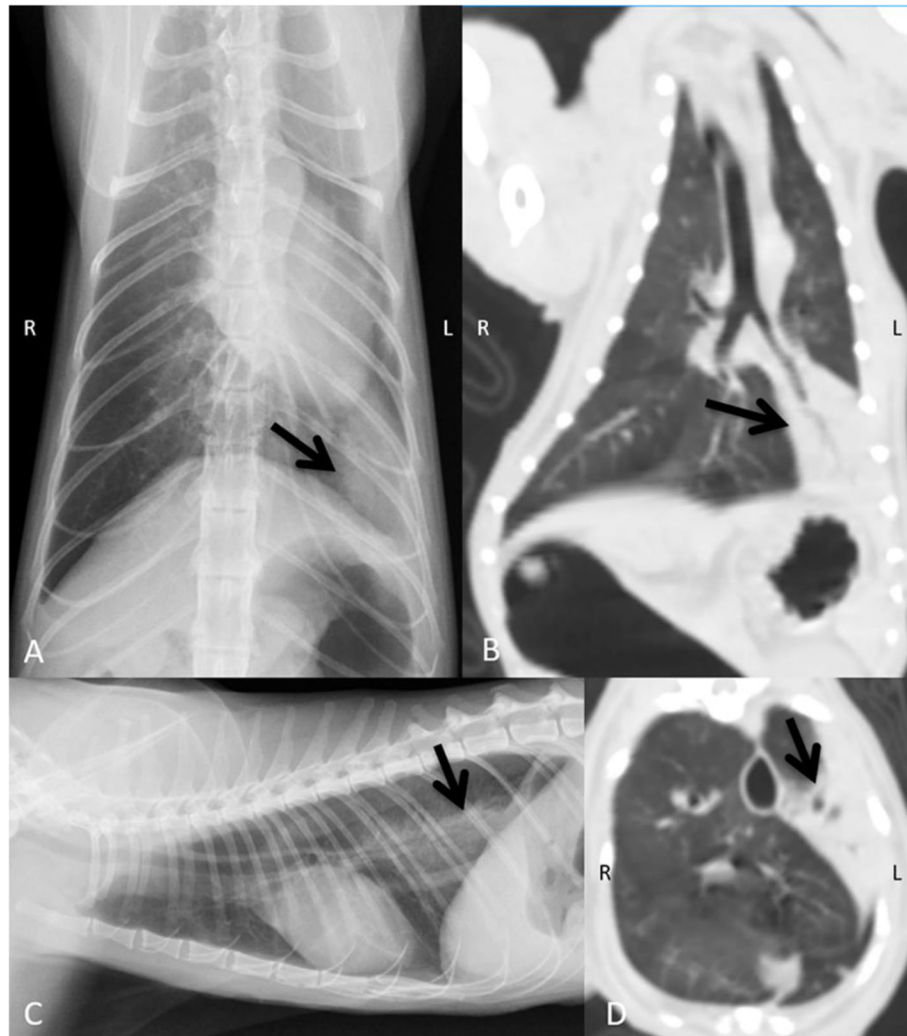


Fig. 2 Ventrodorsal (A) and right lateral (C) thoracic radiographs and dorsal (B) and transverse (D) computed tomographic images of a mammary gland carcinoma affected cat. On thoracic radiograph (A and C), a focal, patchy lung consolidation was found at the left caudal lung lobe (arrows). However, on transverse computed tomographic images (B and D), the location of affected lung parenchyma was revealed as the lobar atelectatic area (arrows)

bronchial area in cats without non-anesthetic methods or without the breath-hold, general anesthesia technique, should be avoided to prevent misinterpretation due to pulmonary atelectasis.

Non-anesthetic, thoracic radiographs and CT were done in MGC-affected cats. Both results can be comparable by means of the status of pulmonary inflation; the positionings for evaluation were different though. Thoracic CT can identify a greater number of lung metastatic affected cats and a higher number of pulmonary nodules of a smaller size compared with thoracic radiographs. Due to the transverse display, CT can reduce the superimposition that provides the greatest impact on assessment of small pulmonary nodules similar to dogs [7]. Ill-defined nodules or diffuse pulmonary patterns observed on thoracic radiography have been reported in

83 % of cats suffering from MGC [29]. However, CT showed a clearer border of those lung nodules as observed in our study. Therefore, the sensitive diagnostic method of CT helps assess the prognostic survival period. It is well known that therapeutic treatment for animals presenting with metastatic lesions is a candidate for poor prognosis and that standard chemotherapy is commonly ineffective [30].

The most frequent locations of lung nodules occurred at the caudal thoracic compartment. Although this area was prone to being affected with motion artifacts in non-anesthetized healthy cats, this motion artifact was unlikely to be seen in the MGC-affected cats. The less motion artifacts at this area could be related to advancing age and health conditions of MGC-affected cats. They were senile and in an unhealthy condition that

may cause a lower respiratory rate compared to young healthy cats, the actual respiratory rates between groups of cats during the CT scan was difficult to detect though. Thus, the utilization of CT without general anesthesia could be superior for evaluating lung metastatic nodules in feline MGC. Moreover, CT provided additional information involving metastatic processes such as sternal lymphadenopathy and pleural effusion, which were more difficult to detect on thoracic radiograph in the case of mild alterations.

Regarding clinical situations in limited circumstances and the regulation of animal use policy, we were unable to perform cytological/histological examination of lung nodules in all feline MGCs. It is possible that some pulmonary nodules were granulomas or lung fibrosis. In addition, in clinical situations, it was difficult to set up an age-match control study to evaluate the lung condition because senile cats are prone to be affected with other diseases related to anesthetic risk. Moreover, in MGC, the comparisons between clinical stages and tissue subtypes could not be done due to the insufficient number of samples. Therefore, the comparison of the diagnostic evidence with histopathology and/or clinical staging warrants further investigation.

Conclusions

General anesthesia clearly resulted in lung atelectasis, particularly of the cranial lung lobe whereas non-anesthetic pulmonary parenchyma on CT showed caudal thoracic motion artifacts. On the other hand, in senile MGC-affected cats, non-anesthetic CT was recommended because it provided less motion artifact and high sensitivity to detecting very small-sized lung nodules including intra-thoracic lymphadenopathy and pleural effusion more clearly than that observed on conventional, non-anesthetic radiographs.

Methods

Animals

This study was divided into two parts: an investigation of the anesthetic effect on lung characteristics in clinically healthy cats and a comparison of diagnostic accuracy between non-anesthetic CT and conventional, non-anesthetic thoracic radiographs for detecting MGC lung lesions. All cats conducting experiments were presented to The Small Animal Hospital, Faculty of Veterinary Science, Chulalongkorn University from January 2017 to February 2020. The study was approved by The Chulalongkorn University Animal Care and Use Committee (CU-IACUC); the approval numbers 1631073, 1831094 and 1931039 for cats in Gr. 1, 2 and 3, respectively. All experiments were carried out in accordance with relevant guidelines and regulations. All owners of

the cats were informed consents and then all consents were written by the the cat owners.

Cats were divided into three groups: group 1 (Gr. 1: the anesthetized healthy cats); group 2 (Gr. 2: the non-anesthetized healthy cats); and group 3 (Gr. 3: MGC-affected cats). The inclusion criteria for cats in Gr. 1 and Gr. 2 were clinically healthy cats showing unremarkable results through history taking, physical examinations, thoracic auscultation, hematology, and basic serum biochemistry, thoracic radiographs and abdominal ultrasound. Cats that revealed any abnormalities from those health screenings were excluded. Gr. 3 were MGC-affected cats that had previous cytologic or histopathologic confirmation of mammary gland adenocarcinoma. Cats that were pregnant, were in lactating period, and had a history or clinical signs of other respiratory such as asthma or previous pneumonia or other intra-thoracic abnormalities unrelated to MGC, e.g. mediastinal abnormality, cardiomegaly, or pleural effusion, were excluded from this study. Clinical demographic information was recorded.

Radiography for MGC-affected cats

Non-anesthetic, thoracic radiographs were performed using the standard institutional procedure. Right lateral, left lateral, and ventrodorsal thoracic radiographs were obtained. In Gr. 3, thoracic radiographs were primarily noted as either positive or negative for lung nodules, enlargement of intrathoracic lymph nodes and evidence of pleural effusion. Subsequently, each lateral radiograph was divided into three compartments of cranial (thoracic inlet to cranial cardiac silhouette), middle (cranial cardiac silhouette to cardiac apex), and caudal parts (cardiac apex to caudodorsal lung area). The number, size, and contour of lung nodules on each view and each area were then recorded. Furthermore, interlobular fissures were observed on the ventrodorsal radiographs for pleural effusion.

Computed tomography

Prior to CT, cats in Gr.1 were sedated using acepromazine maleate (0.03 mg/kg, Combistress, Pharmaceuticals ND) and tramadol hydrochloride (2 mg/kg, Tramache, Harson Laboratories) intramuscularly, followed by induction with propofol (2–4 mg/kg, Propofol-Lipuro 1 % Ampoule, B. Braun) intravenously. After endotracheal intubation, anesthesia was maintained with 2–2.5 % of isoflurane in 100 % oxygen using a pressure controlled-ventilator (SV-2000, SORA MEDICAL TECH) at a rate of 12 breaths/minute, tidal volume at 15 ml/kg and maximal intratracheal pressure at 15 cmH₂O without the breath-hold technique. Pre-contrast enhanced CT was obtained at approximately 10 min after intubation. On the other hand, cats in Gr. 2 and Gr. 3 were manually

restrained in a plastic carrying box and supported by rolled towels for the desired position. As soon as positioning was achieved, CT images were obtained using a 64-slice, multi-detector CT scanner (Optima 660, GE Healthcare). During CT acquisition, all cats were in sternal recumbency with the head pointed into the CT gantry and the thoracic cavity perpendicular to the isocenter of the CT scan planes. Non-contrast enhanced CT was acquired at 120 kilovoltage peak (kVp), auto-mate milliamperage (mA), effective slice thickness at 0.625 mm, collimator pitch at 0.935 mm, matrix size of 512×512 (isotropic voxels) and the field of view (FOV) was set to cover the whole area of the cats or the positioning device. CT images were collected in the Digital Imaging and Communications in Medicine (DICOM) format and analyzed with DICOM image viewer software (Osirix®, Pixmeo SARL).

A pulmonary window at 1400 Hounsfield unit (HU) of window width (WW) and -500 HU of window level (WL) was applied to transverse CT images to evaluate each hemithorax. At first, motion artifacts were evaluated. Motion artifacts were classified into three grades: grade 0 (G0): an absence of image blurring due to respiratory motion; grade 1 (G1): the mild to moderate presence of image blurring that did not influence diagnostic quality; grade 2 (G2): severe presence of image blurring causing poor diagnostic quality [10]. Subsequently, the lung parenchyma was observed for lung atelectasis. The attenuation number at each of right cranial lung lobe (RtCr), right middle lung lobe (RtMd), right caudal lung lobe (RtCa), right accessory lung lobe (RtAcc), cranial part of left cranial lung lobe (LtCrCr), caudal part of left cranial lung lobe (LtCrCa), and left caudal lung lobe (LtCa) was observed by drawing a 5 mm^2 of region of interest (ROI) and comparing them. The ROI was selectively drawn on the lung parenchyma without any distinct pulmonary vessels or airways. Lung was defined as normal lung tissue (NL) if lung attenuation was between -900 and -501 HU; poorly lung aeration (PA) if lung attenuation was between -500 and -101 HU; and non-lung aeration (NA) if lung attenuation was between -100 and 100 HU [20]. Lung atelectasis was noted according to anatomical lobes and intra-parenchymal locations such as peripheral, peribronchial, or diffused patterns. Furthermore, the distribution of lung atelectasis was classified as being in dorsal, ventral or diffuse lung areas.

In Gr. 3, the number, diameters, and contours of lung nodules were observed on the transverse CT image and information was recorded for each area similar to the thoracic radiographs. Intra-thoracic lymphadenopathy and signs of pleural effusion were observed and noted.

Statistical analysis

Descriptive statistics were used to present quantitative clinical demographic data. All statistical comparisons

were conducted using Prism7 (GraphPad Software, San Diego, CA, USA). The normality test for each data set was primarily determined by the Shapiro-Wilk test. Age, BW, and motion artifacts among groups were compared using the Kruskal-Wallis test with Dunn's multiple comparisons test or one-way ANOVA. The attenuation number of lungs between groups of clinically healthy cats was compared using an unpaired t-test whereas the association between anesthetic procedure and the presence of lung atelectasis was evaluated using the odds ratio. In addition, the number of lung nodules including size detected on CT and thoracic radiographs were compared using a Wilcoxon test. $P < 0.05$ was considered statistically significant.

Abbreviations

BW: Body weight; CI: Confidence interval; CT: Computed tomography; CU-ACUC: Chulalongkorn University Animal Care and Use Committee; DICOM: Digital Imaging and Communications in Medicine; FOV: Field of view; Group: Gr; HU: Hounsfield unit; kg: Kilogram; kVp: Kilovoltage peak; LtCa: Left caudal lung lobe; LtCrCa: Caudal part of left cranial lung lobe; LtCrCr: Cranial part of left cranial lung lobe; mA: Milliamperage; mg: Milligram; MGC: Mammary gland carcinoma; mm: Millimeter; NA: Non-lung aeration; NL: Normal lung tissue; OR: Odd ratio; PA: Poorly lung aeration; ROI: Region of interest; RtAcc: Right accessory lung lobe; RtCa: Right caudal lung lobe; RtCr: Right cranial lung lobe; RtMD: Right middle lung lobe; WL: Window level; WW: Window width

Acknowledgements

This study was kindly supported and facilitated by the Diagnostic Imaging Unit, the Small Animal Hospital, Faculty of Veterinary Science, Chulalongkorn University, Bangkok, Thailand.

Authors' contributions

Study conception and design: AK, SP and NC; Acquisition of data: AK, SS, NT, KY, CT and NC; Analysis and interpretation of data: AK, CT, SP and NC; Drafting of manuscript: AK and NC; Critical revision: SP and NC; All authors read and approved the final manuscript.

Funding

This study was supported by the scholarship from the Graduate School of Chulalongkorn University-the 90th anniversary Chulalongkorn University Fund (Ratchadaphiseksomphot Endowment Fund) (Grant number GCGU R1125632151M,151) and by the Faculty of Veterinary Science, Chulalongkorn University, Bangkok, Thailand. The first funder provided financial support for the experiment and the second funder supported the data collection, laboratory equipment and analysis including publication fee.

Availability of data and materials

The datasets used and/or analyzed during the current study are available from the corresponding author on reasonable request.

Declarations

Ethics approval and consent to participate

All procedures involving animals in this study were approved by the Chulalongkorn University Animal Care and Use Committee (CU-IACUC), Faculty of Veterinary Science, Chulalongkorn University (Protocol number: 1631073, 1831094 and 1931039). All experiments were carried out in accordance with institutional guidelines and regulations, and the study was carried out in compliance with the ARRIVE guidelines. All owners were informed consents and gave the written consent for allowing their animals to be parts of this study.

Consent for publication

Not applicable.

Competing interests

The authors declare that they have no competing interests.

Author details

¹Department of Surgery, Faculty of Veterinary Science, Chulalongkorn University, 39 Henri-Dunant Road, Wangmai, Pathumwan, 10330 Bangkok, Thailand. ²Department of Obstetrics, Gynaecology and Reproduction, Research Unit of Obstetrics and Reproduction in Animals, Faculty of Veterinary Science, Chulalongkorn University, 10330 Bangkok, Thailand.

Received: 24 March 2021 Accepted: 29 June 2021

Published online: 06 July 2021

References

- Hassan BB, Elshafae SM, Supsavhad W, Simmons JK, Dirksen WP, Sokkar SM, Rosol TJ. Feline mammary cancer: novel nude mouse model and molecular characterization of invasion and metastatic genes. *Vet Pathol*. 2017;54(1):32–43.
- Manuali E, Forte C, Vichi G, Genovese DA, Mancini D, De Leo AAP, Cavicchioli L, Pierucci P, Zappulli V. Tumours in European shorthair cats: a retrospective study of 680 cases. *J Feline Med Surg*. 2020;22(12):1095–1102.
- Mills SW, Musil KM, Davies JL, Hendrick S, Duncan C, Jackson ML, Kidney B, Pillibert H, Wobeser BK, Simko E. Prognostic value of histologic grading for feline mammary carcinoma: a retrospective survival analysis. *Vet Pathol*. 2015;52(2):238–249.
- Zappulli V, Rasotto R, Caliarì D, Mainenti M, Peña L, Goldschmidt MH, Kiupel M. Prognostic evaluation of feline mammary carcinoma: a review of the literature. *Vet Pathol*. 2015;52(1):46–60.
- Hayes AA, Mooney S. Feline Mammary Tumors. *Vet Clin North Am Small Anim Pract*. 1985;15(3):513–520.
- Hann KA, Bravo L, Avenell JS. Feline breast carcinoma as a pathologic and therapeutic model for human breast cancer. *In Vivo*. 1994;8(5):825–828.
- Nemanic S, London CA, Wisner ER. Comparison of thoracic radiographs and single breath-hold helical CT for detection of pulmonary nodules in dogs with metastatic neoplasia. *J Vet Intern Med*. 2006;20(3):508–515.
- Otoni CC, Rahal SC, Vulcano LC, Ribeiro SM, Hette K, Giordano T, Doiche DP, Amorim RL. Survey radiography and computerized tomography imaging of the thorax in female dogs with mammary tumors. *Acta Vet Scand*. 2010; 52(1):20.
- Oliveira CR, Mitchell MA, O'Brien RT. Thoracic computed tomography in feline patients without use of chemical restraint. *Vet Radiol Ultrasound*. 2011;52(4):368–376.
- Masseau I, Reinero CR. Thoracic computed tomographic interpretation for clinicians to aid in the diagnosis of dogs and cats with respiratory disease. *Vet J*. 2019;253:105388.
- Lin CH, Lo PY. Simple technique for aiding thoracic CT scanning of cats without general anaesthesia. *Vet Rec*. 2018;182(7):197.
- Collins SP, Matheson JS, Hamor RE, Mitchell MA, Labelle AL, O'Brien RT. Comparison of the diagnostic quality of computed tomography images of normal ocular and orbital structures acquired with and without the use of general anesthesia in the cat. *Vet Ophthalmol*. 2013;16(5):352–358.
- Miskovic A, Lumb AB. Postoperative pulmonary complications. *Br J Anaesth*. 2017;118(3):317–334.
- Thrall DE. Principles of radiographic interpretation of the thorax. In: Thrall DE. *Textbook of Veterinary Diagnostic Radiology*. 6th ed. St Louis, MO: Elsevier, 2015;474–488.
- Brismar B, Hedenstierna G, Lundquist H, Strandberg A, Svensson L, Tokick L. Pulmonary densities during anesthesia with muscular relaxation - a proposal of atelectasis. *Anesthesiology*. 1985;62(4):422–428.
- Ahlberg NE, Hoppe F, Kelter U, Svensson L. A computed tomographic study of volume and x-ray attenuation of the lungs of beagles in various body positions. *Vet Radiol Ultrasound*. 1985;26(2):43–47.
- Le Roux C, Cassel N, Fosgate GT, Zwingenberger AL, Kirberger RM. Computed tomographic findings of pulmonary atelectasis in healthy anesthetized Beagles. *Am J Vet Res*. 2016;77(10):1082–1092.
- Littleton SW, Tulaimat A. The effect of obesity on lung volumes and oxygenation. *Respir Med*. 2017;124:15–20.
- Hedenstierna G, Tokics L, Scaramuzzo G, Rothen HU. Oxygenation impairment during anesthesia: influence of age and body weight. *Anesthesiology*. 2019;131:46–57.
- Masseau I, Banuelos A, Dodam J, Cohn LA, Reinero C. Comparison of lung attenuation and heterogeneity between cats with experimentally induced allergic asthma, naturally occurring asthma and normal cats. *Vet Radiol Ultrasound*. 2015;56(6):595–601.
- Hornby N, Lamb CR. Does the computed tomographic appearance of the lung differ between young and old dogs? *Vet Radiol Ultrasound*. 2017;58(6): 647–652.
- Magnusson L, Spahn DR. New concepts of atelectasis during general anesthesia. *Br J Anaesth*. 2003; 91: 61–72.
- Hedenstierna G, Edmark L. Mechanisms of atelectasis in the perioperative period. *Best Pract Res Clin Anaesthesiol*. 2010;24(2):157–169.
- Reber A, Nyland U, Hedenstierna G. Position and shape of the diaphragm: implications for atelectasis formation. *Anaesthesia*. 1998;53(11):1054–1061.
- Staffieri F, Franchini D, Carella GL, Montanaro MG, Valentini V, Driessen B, Grasso S, Crovace A. Computed tomographic analysis of the effects of two inspired oxygen concentrations on pulmonary aeration in anesthetized and mechanically ventilated dogs. *Am J Vet Res*. 2007;68(9):925–931.
- Staffieri F, De Monte V, De Marzo C, Grasso S, Crovace A. Effects of two fractions of inspired oxygen on lung aeration and gas exchange in cats under inhalant anaesthesia. *Vet Anaesth Analg*. 2010;37(6):483–490.
- Lamb CR, Jones ID. Association between respiratory signs and abnormalities reported in thoracic CT scans of cats. *J Small Anim Pract*. 2016;57(10):561–567.
- Lee SK, Park S, Cheon B, Moon S, Hong S, Cho H, Chang D, Choi J. Effect of position and time held in that position on ground-glass opacity in computed tomography images of dogs. *Am J Vet Res*. 2017;78(3):279–288.
- Forrest LJ, Graybush CA. Radiographic patterns of pulmonary metastasis in 25 cats. *Vet Radiol Ultrasound*. 1998;39(1):4–8.
- Ogilvie GK, Straw RC, Jameson VJ, Walters LM, Lafferty MH, Powers BE, Withrow SJ. Evaluation of single-agent chemotherapy for treatment of clinically evident osteosarcoma metastases in dogs: 45 cases (1987–1991). *J Am Vet Med Assoc*. 1993; 202(2):304–306.

Publisher's Note

Springer Nature remains neutral with regard to jurisdictional claims in published maps and institutional affiliations.

Ready to submit your research? Choose BMC and benefit from:

- fast, convenient online submission
- thorough peer review by experienced researchers in your field
- rapid publication on acceptance
- support for research data, including large and complex data types
- gold Open Access which fosters wider collaboration and increased citations
- maximum visibility for your research: over 100M website views per year

At BMC, research is always in progress.

Learn more biomedcentral.com/submissions

